Impact of Artificial Reservoir Water Impoundment on Global Sea Level

B. F. Chao,* Y. H. Wu, Y. S. Li

By reconstructing the history of water impoundment in the world's artificial reservoirs, we show that a total of ~10,800 cubic kilometers of water has been impounded on land to date, reducing the magnitude of global sea level (GSL) rise by −30.0 millimeters, at an average rate of −0.55 millimeters per year during the past half century. This demands a considerably larger contribution to GSL rise from other (natural and anthropogenic) causes than otherwise required. The reconstructed GSL history, accounting for the impact of reservoirs by adding back the impounded water volume, shows an essentially constant rate of rise at +2.46 millimeters per year over at least the past 80 years. This value is contrary to the conventional view of apparently variable GSL rise, which is based on face values of observation.

The various causes of the observed global sea level (GSL) rise have been under study, and debate, for years. The Intergovernmental Panel on Climate Change (*1*) concluded in 2007 that "the budget (of GSL rise) has not yet been closed satisfactorily," primarily because the anthropogenic contribution from land water alterations is too poorly known. Among them, the negative contribution due to water impoundment in artificial reservoirs behind dams has long been recognized to be a major term (*1*–*7*), although one poorly quantified in the absence of compiled information. Such incomplete data have led to a wide range of estimates of the total water impoundment: from ~15,000 km^3 (extrapolated to year 2000) (*2*) to ~10,000 km^3 (*3*) [which includes the volume of only the "top 100" (named) reservoirs, ~4000 km^3 (*4*)] to 5000 to 6000 km^3 (*5*–*7*) and even less (*8*).

To reconstruct the water impoundment history and study its impact on GSL rise, we assembled a comprehensive tally of the world's reservoirs constructed since ~1900. Our main source of data was the International Commission on Large Dams (ICOLD) World Register of Dams (*9*), augmented and corrected for apparently erroneous or inconsistent entries by consulting with various ancillary data sources (*10*–*16*) to yield a list of 29,484 named reservoirs with nominal capacity and year of completion (*17*).

Let $V(t)$ be the (cumulative) total volume of water impoundment in the world's reservoirs at any given calendar year t, and let V_i be the capacity of a given individual reservoir modeled as an addition to V in year t_i of its completion, causing an instantaneous GSL drop (recognizing the ocean as the ultimate source of the water). That is, $V(t) = \Sigma_i V_i H(t - t_i)$ and the corresponding GSL drop $d(t) = -V(t)/A$ (a negative value), where H is the Heaviside function and $A = 3.61 \times 10^8$ km^2 is the total ocean area. This "nominal" time history for $V(t)$ is shown in Fig. 1 (dashed blue curve); the total nominal V to date is 8300 km^3, corresponding to $d = -23$ mm. The inset shows the number of reservoirs completed per year, which has soared since ~1950 but distinctly decreased in the past three decades, especially in North America and Europe, because of environmental concerns. The slowdown during the Second World War is also noted (see below). In addition, the continental breakdown in Fig. 1 reflects the contrasting and changing societal behavior and economic activity of populations on different continents.

Next, the following potentially important modifications to the nominal history above should be considered.

First, although our tally of reservoirs is essentially complete for the major and relatively large ones, the tally inevitably becomes less complete with decreasing reservoir size as those reservoirs become more numerous. We assess the untallied amount of water as follows. We plot in Fig. 2 the histogram of the number of tallied reservoirs n (in logarithm) versus a convenient reservoir "magnitude" $M = \log(C)$, where C is the reservoir capacity in cubic meters. The drop-off of the tally of n is found to occur around $M \sim 6.5$ (corresponding to a moderate reservoir of, say, 1 km long, 150 m

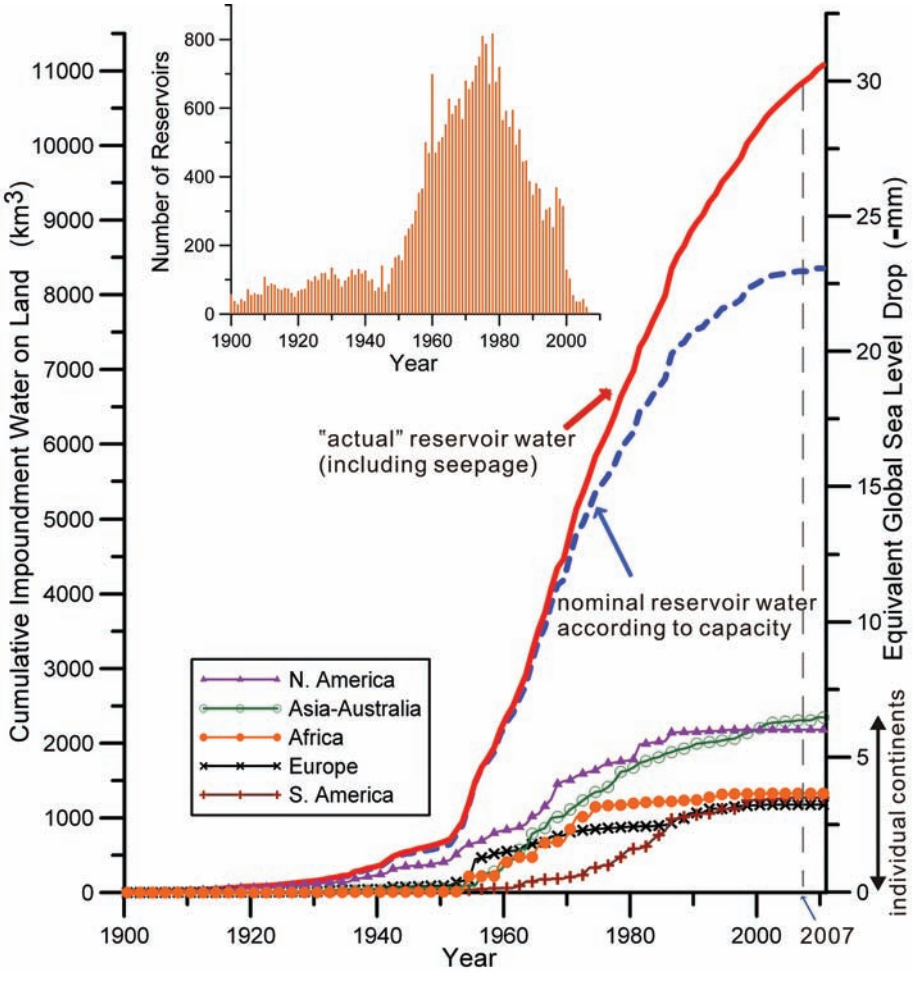

Fig. 1. Cumulative water impoundment [$V(t)$, red solid curve] as a function of calendar year, based on the nominal water impoundment (dashed blue curve) according to our compiled tally of 29,484 reservoirs' capacity (*17*) but also including realistic modifications to account for phenomena such as subsurface seepage. The lower thin lines are the breakdowns for individual continents, showing continental contrasts. The inset shows the number of reservoirs completed per year.

College of Earth Sciences, National Central University, Chung-Li, Taiwan, ROC.

*To whom correspondence should be addressed. E-mail: bfchao@ncu.edu.tw

wide, and 20 m deep). Over the main body of the histogram for $M > 6.5$ (numbering 16,600 reservoirs), up to $M = 10.5$ with bin width of 0.1, the (log-log) relation conforms to a straight line corresponding to an empirical power law: $n(C) = 10^{6.69} \times C^{-0.52}$ (*18*). Extrapolating to zero capacity, this relation yields the integrated water amount for all reservoirs smaller than $M = 6.5$, which amounts to only 0.73%, to be augmented to the total (*19*, *20*). This reassures us that our tally's incompleteness in small reservoirs is inconsequential with respect to total water volume.

Second, accounting only for the "visible" part of the impounded water, the nominal V_i ignores the water that inevitably seeps underground to manifest as water table elevation. Typically comparable to the capacity, the volume of this invisible subsurface water varies greatly from case to case, depending on the local geology and climate. Short of detailed information, here we make an average, conservative estimate: For all reservoirs we assume an annual subsurface seepage rate of 5% of the capacity volume for the first year of existence (*6*). For the out-years following (*21*), we use a dynamic fluid diffusion model that dictates the water seepage to decrease as $1/\sqrt{t}$, so that the total water seepage grows slowly as $\sqrt{t}$. We then integrate this seepage into the total volume accordingly.

Third, reservoirs are not always filled to 100% of V_i. Depending on the usage and the regional climatology and hydrology, actual reservoir storage can fluctuate considerably, especially seasonally and often interannually. Here, following (*6*), we adopt a long-term average percentage of 85% and thus an overall scale factor of 0.85. Incidentally, to first order, the inevitable silting of reservoirs need not be of concern here [contrary to (*5*–*7*)] because, just like water, the silt represents that much volume withheld on land that would otherwise flow to the ocean, raising GSL. Whether the volume withheld by the dam is water or silt has the same impact on GSL.

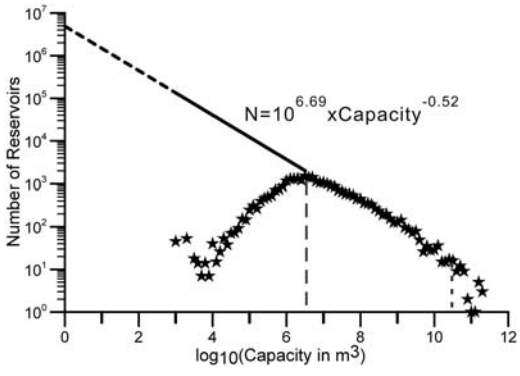

Fig. 2. Histogram of the number of tallied reservoirs (in logarithm) versus the reservoir magnitude $M = \log(C)$, where C is the reservoir capacity in units of m^3 of volume. Over the main body of the histogram for $M = 6.5$ to 10.5, the (log-log) relation conforms to a straight line with slope –0.52.

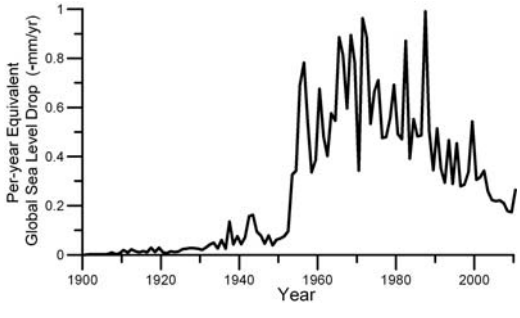

Fig. 3. History of annual GSL drop due to water impoundment in artificial reservoirs.

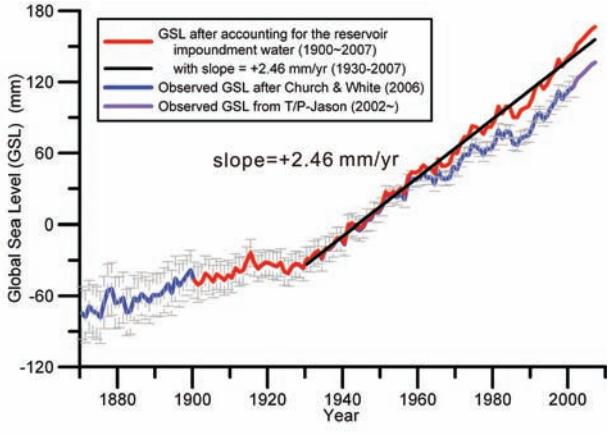

Fig. 4. The blue curve with error bar is the observed GSL history [(*1*, *25*); zero level is arbitrary], with a purple segment from altimetry data (*23*) spliced on for the past few years after adjusting a vertical offset. The red line is the GSL corrected for the impact of artificial reservoirs, reconstructed by adding back the reservoir impoundment contribution (in Fig. 1) to the blue curve. It exhibits an essentially constant slope of +2.46 mm/year for the past 80 years.

Combining the above, a modified water impoundment curve for $V(t)$ and $d(t)$ (solid red curve in Fig. 1) emerges from the nominal curve. The total actual water impoundment to date is $V =$ 10,800 km^3, corresponding to $d = -30.0$ mm (*22*). Figure 3 shows the annual GSL drop [essentially the time derivative of $V(t)$]; in peak years, ~1960 to 1990, it reached as high as –0.4 to –0.9 mm/year. The average GSL drop rate during the past half century is about –0.55 mm/year.

Sea level varies on all temporal and spatial scales for a host of reasons. Tide gauge data indicate that GSL has risen at +1.7 to 1.8 mm/year during the 20th century [(*1*) and references therein], whereas satellite altimetry during 1993–2007 shows an accelerated rate of +3.36 ± 0.4 mm/year (*23*), although it is uncertain whether this is a long-term trend or decadal variability (*1*). One-quarter to one-half of the rise in the past half century is believed to have come from the thermal expansion of the top layers of global oceans (the steric effect). The rest, barring a relatively small but uncertain portion from the mantle glacial isostatic adjustment, is attributed to water mass addition occurring in two forms: (i) melting of mountain glaciers (estimated contribution to GSL rise: +0.50 ± 0.18 mm/year during 1961–2003 and +0.77 ± 0.22 mm/year during 1993–2003) plus that of the ice sheets on Antarctica (+0.14 ± 0.41 mm/year and +0.21 ± 0.35 mm/year, respectively) and Greenland (+0.05 ± 0.12 mm/year and +0.21 ± 0.07 mm/year, respectively), and (ii) climate-driven variations in soil water, inland seas, and large lakes (+0.12 mm/year during the past two decades, although with large interannual and decadal fluctuations), plus various anthropogenic contributions including the impoundment under study here.

Thus, our estimate of a difference of –0.55 mm/year due to artificial reservoirs represents a considerable (negative) impact to the GSL rise budget for the past several decades, which has more than compensated for nearly all of the individual natural or anthropogenic (positive) contributions described above (*24*). This creates an even larger gap in the GSL rise budget, demanding a larger contribution from the natural (and perhaps anthropogenic) causes than otherwise required.

Equally important, our study has intriguing implications for the history of GSL rise, a key indicator of global climatic change. In Fig. 4 we plot the observed GSL history (*1*, *25*) as the blue line, with a splice-on segment for the most recent decade derived from the altimetry result (*23*) (the purple segment) after adjusting a vertical offset to match the former. That curve implies that the observed GSL rise during the past century has been variable in a piecewise manner: A slower section before ~1930 is followed by a faster section until ~1960, with a slower section again extending until ~1990 before becoming faster again. We suggest that this seeming variability in rate is "artificial." If we add back the actual $V(t)$ in Fig. 1 to reconstruct

a GSL curve, giving the GSL variation that would have been free from the impact of artificial reservoirs, it becomes evident that, in contrast to the observations, the post-1930 GSL rose essentially at a constant rate all the way to the recent years (barring any interspersed interannual fluctuations such as El Niño–Southern Oscillation events or volcanic activities) at a rate of +2.46 mm/year, versus an average of +1.7 to 1.8 mm/year during the 20th century with recent acceleration. Whether this means that the global changes causing the GSL rise have been in operation in a rather steady fashion, or instead fortuitously compensated one another over at least the past 80 years, remains to be examined.

Our findings differ from the conventional wisdom, which holds an apparent variable GSL rise according to the face values of observation as stated above. This, of course, by no means precludes the most recent or possible future acceleration of GSL rise (*23*) due to natural causes, compounded by the further slowdown of reservoir-building in the near future (*26*).

References and Notes

1. N. L. Bindoff *et al.*, in *Climate Change 2007: The Physical Science Basis. Contribution of Working Group I to the Fourth Assessment Report of the Intergovernmental Panel on Climate Change*, S. Solomon *et al.*, Eds. (Cambridge Univ. Press, New York, 2007), chap. 5.
2. W. S. Newman, R. W. Fairbridge, *Nature* **320**, 319 (1986).
3. B. F. Chao, *Eos* **72**, 492 (1991).
4. B. F. Chao, *Geophys. Res. Lett.* **22**, 3533 (1995).
5. V. Gornitz, C. Rosenzweig, D. Hillel, *Global Planet. Change* **14**, 147 (1997).
6. V. Gornitz, in *Sea Level Rise*, B. Douglas, M. Kearney, S. Leatherman, Eds. (Academic Press, London, 2001).
7. D. L. Sahagian, *Global Planet. Change* **25**, 39 (2000).
8. D. L. Sahagian, F. W. Schwartz, D. K. Jacobs, *Nature* **367**, 54 (1994).
9. *World Register of Dams* (International Commission on Large Dams, Paris, 2007) (www.icold-cigb.net).
10. F. van der Leeden, *Water Resources of the World* (Water Information Center Inc., New York, 1975).
11. *World Water Balance and Water Resources of the Earth* (UNESCO, Paris, 1978).
12. U.S. Department of the Interior, *Major Dams, Reservoirs, and Hydroelectric Plants* (Bureau of Reclamation, Denver, 1983).
13. *International Water Power & Dam Construction Handbook*, R. M. Taylor, Ed. (Reed Business, Surrey, UK, 1993).
14. World Commission on Dams, *Dams and Development* (Earthscan, London, 2000).
15. UNESCO, *World Water Resources at the Beginning of the 21st Century* (Cambridge Univ. Press, New York, 2003).
16. W. W. Storage, *in Man-Made Reservoirs* (Foundation for Water Research, Marlow, UK, 2005).
17. See supporting material on *Science* Online.
18. Different (least-squares) fit ranges and bin widths were tried; the results vary little.
19. The rapid convergence of the extrapolated integration, consistent with (*20*), down to small reservoir size is assured as follows. For a self-similar fractal "map" distribution of self-similar reservoirs with respect to the linear dimension L, the reservoir number decreases as L^{-2} while the corresponding volume increases as L^3. Hence, the water impoundment for a given size increases as L, dominated by large reservoirs. The actual reservoir number increases with smaller size even more slowly than the above, only at $L^{-1.56}$ ($-1.56 = -0.52 \times 3$). The situation is analogous to the (Richter-Gutenberg) frequency-moment relationship for seismicity, where the "β value" (or the negative of the power-law slope) is ⅔, hence the total seismic energy release is dominated by large earthquakes even though the smaller earthquakes are much more numerous.
20. M. I. L'vovich, G. F. White, in *The Earth as Transformed by Human Action*, B. L. Turner II *et al.*, Eds. (Cambridge Univ. Press, Cambridge, 1990).
21. P. C. D. Milly *et al.*, position paper, World Climate Research Programme Workshop on Understanding Sea-Level Rise and Variability (UNESCO, Paris, 2006).
22. By comparison, in terms of GSL the total atmospheric water content is equivalent to ~35 mm and the total biological water is equivalent to ~3 mm.
23. B. D. Beckley, F. G. Lemoine, S. B. Luthcke, R. D. Ray, N. P. Zelensky, *Geophys. Res. Lett.* **34**, L14608 (2007).
24. Among other anthropogenic (positive) contributions to GSL, groundwater mining (mainly for irrigation) is potentially important (*1*, *5*–*7*), which partially offsets the impact of the reservoir impoundment. Its amount is considerably smaller (*6*), albeit far less certain, than the reservoirs', and presumably grew over the decades with a different time signature. A separate assessment is needed.
25. J. A. Church, N. J. White, *Geophys. Res. Lett.* **33**, L01602 (2006).
26. The slowdown is already evident in Fig. 1, which includes the projection into the next few years according to our tally (for example, $d = -30.6$ mm by 2010), although late reporting of reservoir-building may have also contributed to the apparent slowdown.

27. We thank J. Church, R. Ray, D. Sahagian, A. Cazenave, C. K. Shum, L. Y. Tsai, S. T. Li, and L. Lin for discussions and assistance. Supported by the Taiwan Semiconductor Manufacturing Company Ltd. Chair professorship and by National Science Council of Taiwan grant NSC96-2111-M-008-016-MY2.

Supporting Online Material

www.sciencemag.org/cgi/content/full/1154580/DC1
Materials and Methods
Table S1

26 December 2007; accepted 5 March 2008
Published online 13 March 2008;
10.1126/science.1154580
Include this information when citing this paper.

Determining Chondritic Impactor Size from the Marine Osmium Isotope Record

François S. Paquay,[1]* Gregory E. Ravizza,[1] Tarun K. Dalai,[1]† Bernhard Peucker-Ehrenbrink[2]

Decreases in the seawater $^{187}Os/^{188}Os$ ratio caused by the impact of a chondritic meteorite are indicative of projectile size, if the soluble fraction of osmium carried by the impacting body is known. Resulting diameter estimates of the Late Eocene and Cretaceous/Paleogene projectiles are within 50% of independent estimates derived from iridium data, assuming total vaporization and dissolution of osmium in seawater. The variations of $^{187}Os/^{188}Os$ and Os/Ir across the Late Eocene impact-event horizon support the main assumptions required to estimate the projectile diameter. Chondritic impacts as small as 2 kilometers in diameter should produce observable excursions in the marine osmium isotope record, suggesting that previously unrecognized impact events can be identified by this method.

Terrestrial and lunar impact craters, as well as impact debris in the sediment record, reveal that Earth has been struck by asteroids many times throughout its history. However, it is difficult to estimate the size of the impacting bodies, and it is likely that many impacts remain unrecognized because of the continuous reshaping of Earth's surface. Rough estimates of projectile size result from inventories of excess Ir (*1*), called Ir fluences (nanograms per square centimeter), and from models of impact-crater formation (*2*). The former approach involves averaging many individual fluence estimates to obtain a meaningful global signal (*3*–*5*), whereas the latter approach requires that an impact crater be preserved.

Since the first application of the Os isotopic system to the study of impact events (*6*), this system has been extensively applied to estimating the contribution of the projectile to impact breccias and impact melts (*7*). These studies report high Os concentrations and low $^{187}Os/^{188}Os$ ratios of the projectile compared with the target rock, demonstrating that Os isotopes are very sensitive tracers of the presence of residual projectile material. Most previous Os isotope studies of impact events have focused narrowly on the impact horizon (*6*–*11*). However, Os isotope studies of the marine sediment record that span longer time intervals show that the dissolution of impact-derived Os in seawater lowers the $^{187}Os/^{188}Os$ values of the global ocean (*12*, *13*).

We show here that impact-induced excursions in the marine Os isotope record can be used to estimate chondritic impactor size (*14*). These excursions can be understood as the result of mixing ambient seawater Os (characterized by relatively high $^{187}Os/^{188}Os$) with meteoritic Os [with low $^{187}Os/^{188}Os$ (*15*)] that is vaporized on impact and subsequently dissolved in seawater. This interpretive framework allows for the estimation of

[1]Department of Geology and Geophysics, University of Hawaii, Honolulu, HI 96822–2225, USA. [2]Department of Marine Chemistry and Geochemistry, Woods Hole Oceanographic Institution, Woods Hole, MA 02543, USA.

*To whom correspondence should be addressed. E-mail: paquay@hawaii.edu

†Present address: Department of Geology and Geophysics, Indian Institute of Technology, Kharagpur 721302, India.